Electron Transfer Enhanced by Minimal Energy Offset at Organic Semiconductor Interface

Hiroto Iwasaki[1,2], Keisuke Fujimoto[3*], Koki Banno[3], Qing-jun Shui[1], Yutaka Majima[1], Masaki Takahashi[3], Seiichiro Izawa[1,4*]

[1]Laboratory for Materials and Structures, Tokyo Institute of Technology, 4259 Nagatsuta-cho, Midori-ku, Yokohama, Kanagawa 226-8503, Japan. [2]Applied Chemistry Program, Graduate School of Advanced Science and Engineering, Hiroshima University, 1-4-1 Kagamiyama, Higashi-Hiroshima, Hiroshima 739-8527, Japan, [3]Department of Applied Chemistry, Faculty of Engineering, Shizuoka University, 3-5-1 Johoku, Naka-ku, Hamamatsu, Shizuoka, 432-8561, Japan. [4]Precursory Research for Embryonic Science and Technology (PRESTO), Japan Science and Technology Agency (JST), 4-1-8 Honcho, Kawaguchi, Saitama 332-0012, Japan.

E-Mail: izawa.s.ac@m.titech.ac.jp (S.I.), fujimoto.keisuke@shizuoka.ac.jp (K.F.).

Abstract

Enhancing electron transfer between excited states and reducing their energy offset is generally in a trade-off relation, which must be overcome to develop efficient optoelectronic devices. In this study, we systematically investigated, through the analysis of 45 combinations, how to facilitate the electron transfer from the charge transfer (CT) state at the donor/acceptor interface to the triplet

excited state of the emitter to improve the triplet-triplet annihilation emission in organic light-emitting diodes (OLEDs). Our analysis, based on the experimental device properties, revealed that the electron transfer is enhanced by the strong CT interaction and, more importantly, by the minimal energy offset (<0.1 eV). This relation was found to be explained by semi-classical Marcus theory with a small reorganization energy of below 0.1 eV. Furthermore, our analysis led to the discovery of a novel donor/acceptor combination for OLED, yielding an efficient blue emission with an extremely low turn-on voltage of 1.57 V.

Introduction

Electron transfer is one of the most fundamental processes that dominates not only chemical reactions[1,2], but also processes in electronic devices[3,4] and living organisms[5,6]. Marcus theory was proposed more than 60 years ago[7]. This is the basic theory of electron transfer and explains the rates of electron transfer between the electron donor and acceptor species based on their energetics and structures. It has been extensively studied in the fields of chemiluminescence[8] and electrode reaction[9] in solution, and provides essential knowledge that electron transfer occurs most rapidly when the energy difference between the initial and final states is equal to the reorganization energy of the media, as shown in **Fig. 1a**. Organic optoelectronic devices such as organic light-emitting diodes (OLEDs) and organic photovoltaics (OPVs) have been commercialized in the last decades. These devices have many advantages compared to conventional electronic devices. For example, OLEDs are lighter and have a higher contrast ratio than liquid crystal displays (LCDs) [10], and OPVs have lightweight and flexible features in contrast to silicon PVs[11]. The efficiency of organic optoelectronic devices is determined by sequential electron transfer steps at the solid interface between two organic molecules[12,13]. A key intermediate for these steps is the charge transfer (CT) state, which is a weakly bound electron-hole pair by Coulomb attraction at the interface[14,15]. Charge separation and recombination loss in OPVs and recombination emission in OLEDs typically occur through the CT state[16,17]. Enhancing device performance requires the elucidation of energetic and structural factors, which could be achieved by studying electron transfer reactions from the CT state to other excited

states using Marcus theory based on experimental device performance[18–20]. However, the scope of analyses based on experimental device performance remains limited[21] due to multiple influencing factors other than electron transfer reactions, including the device structure, film morphology, and electron injection and transport characteristics[22].

Recently, we have developed upconversion (UC)-OLED by utilizing the electron transfer from the CT state to the triplet excited state (T_1) and the subsequent triplet-triplet annihilation (TTA)[23,24]. The electron transfer steps are illustrated in **Fig. 1b**. TTA could double the energy of the excited state; therefore, the turn-on voltage of the blue UC-OLED was greatly reduced to less than 1.5 V, which is much lower than the typical value of 3 V in conventional blue OLEDs[12]. Using low-energy intermediates at the interface is considered a possible solution to the problems of blue OLEDs, such as a high driving voltage and low stability[12,25]. Another unique feature of UC-OLEDs is that CT and TTA emissions appear at different wavelengths without overlap, because the energies of these states are far apart. This feature is helpful for extracting the energetics and structural factors of these states and for simultaneously analyzing the device efficiency and the electron transfer step between CT to T_1 based on Marcus theory. These analyses could lead not only to efficient blue UC-OLEDs but also to an understanding of other devices, such as OPVs, which include the electron transfer step in the operating mechanism.

In this study, we systematically investigated the electron transfer efficiency from the CT state at the interface to T_1 of the donor (TTA emitter) molecule in 45 UC-OLED devices with combinations

of 3 donor (TTA emitter) materials and 15 acceptors (**Fig. 1c**). The transition from the CT state to T_1 is a single electron transfer step from the lowest unoccupied molecular orbital (LUMO) of the acceptor to LUMO of the donor from a molecular point of view at the solid interface[26]. The energy of the CT state is mainly determined by the energy level difference between the highest occupied molecular orbital (HOMO) of the donor and LUMO of the acceptor[27]. The 45 combinations exhibited various CT state energies owing to their different energy levels. Additionally, different chemical structures result in different orientations and distances at the interface. Therefore, a variety of CT state energies and geometries provides a model study of how to facilitate electron transfer from the CT state to T_1 based on Marcus theory. Through the analysis of 45 combinations, it was found that the electron transfer from the CT state to T_1 is enhanced by a minimal energy offset of less than 0.1 eV. Thanks to the analysis of the electron transfer at the interface, we achieved the highest EQE of up to 4% among blue OLEDs with a turn-on voltage of less than 2.4V reported to date.

Results and Discussion

The chemical structures and the energy levels of the materials used in this work are listed in **Fig. 1c**. We chose 3 anthracene derivatives; 1,2-ADN (9-(Naphthalen-1-yl)-10-(naphthalen-2-yl)anthracene), PCAN (9-(9-Phenylcarbazole-3-yl)-10-(naphthalene-1-yl)anthracene), and TPA-An-mPhCz (4-(10-(3-(9H-carbazol-9-yl)phenyl) anthracen-9-yl)-N,N-diphenylaniline), as donors (TTA emitters) in our UC-OLED devices. The HOMO levels of these three molecules become shallower in

the order of 1,2-ADN, PCAN, and TPA-An-mPhCz depending on the nature of electron-donating groups such as carbazole and triphenyl amine. Anthracene derivatives are known as one of the most widely used host materials in blue fluorescent OLEDs and TTA emitters[28–30]. They satisfy the energy requirements for efficient TTA: their energy levels of T_1 (about 1.7 eV) are slightly higher than one-half of their energy levels of S_1 (about 2.9 eV)[31–33]. As acceptor materials to form D/A interface with donors (TTA emitters), we selected 15 naphthalene diimide (NDI) derivatives with different side chains. NDI derivatives are widely used in OPV field due to their strong electron acceptability[34]. The introduction of different side chains into the NDI backbone can result in different energy levels, molecular orientations, and distance with donor materials (TTA emitters)[23], making it suitable for systematic comparison of the effect of energetic and structural factors on luminescence and electron transfer efficiency in UC-OLEDs. In this work, a layer structure of donor and acceptor was used for the OLED devices as shown in **Fig. 2a**. The device fabrication methods are described in Supplementary Information.

Fig. 2b, c show the *J*-*V* and *L*-*V* characteristics and the EL spectrum of a typical UC-OLED using PCAN and NDI-PhE as donor and acceptor, respectively. With the appropriate combination, blue emission is observed below 1.5 V. In the EL spectrum, TTA-UC emission appears around 450 nm from the anthracene derivatives and CT emission appears around 700 nm from the D/A interface. The difference in the CT state energy of the D/A combinations caused large differences in the

emission intensity of TTA-UC and CT emissions. The device performances of other 44 combinations are summarized in the Supplementary information.

To investigate an electron transfer from CT state to T_1 for efficient TTA-UC emission to occur, we focused on the relation between the energy level of the CT states and the luminescence efficiency. Based on the emission mechanisms of UC-OLEDs, the energy levels of CT states are expected to have a significant effect on the efficiency of electron transfer from CT to T_1 and thus on the luminescence efficiency. To determine the relation between CT state energy and TTA-UC emission efficiency, the maximum EQE of TTA-UC emission (EQE_{max}) was plotted as a function of the CT state energy (E_{CT}) for the devices of each donor (TTA emitter) (**Fig. 3a-c**). The reason why the EQE_{max} is used here rather than the EQE at constant current flow is that the TTA efficiency becomes constant and the EQE_{max} is obtained when the concentration of T_1 are enough high[35]. The CT state energies were calculated by CT emission peak wavelength in EL spectra. In general, the energy difference between singlet and triplet CT states at the interface is negligible[20]. Thus, we do not distinguish the two states. In 1,2-ADN-based devices in **Fig. 3a**, negative correlation was observed. The highest EQE_{max} value was observed in the 1,2-ADN/HF device with the CT state energy of 1.71 eV. In other words, the EQE_{max} increases as the CT state energy decreases. However, in TPA-An-mPhCz-based devices in **Fig. 3c**, the opposite correlation was observed as in case of 1,2-ADN. The TPA-An-mPhCz/EP device with the CT state energy of 1.73 eV showed the highest EQE_{max} value. Meanwhile, the relation between the CT state energy and EQE_{max} appeared as an upward convex

curve in PCAN-based devices (**Fig. 3b**); the emission efficiencies decreased as one moves away from the value of optimal E_{CT} at the center of the curve. The PCAN/PhE device had the highest EQE_{max} of 0.81% among all the 45 combinations, with the CT state energy of 1.75 eV. Here, we combine three plots (**Fig. 3a-c**) using different three donors into one to show the luminescence efficiencies as a function of E_{CT} for all the 45 devices (**Fig. S11**). In order to compare different TTA emitters simultaneously, the luminescence efficiencies were calculated by dividing the EQE_{max} by the photoluminescence quantum yield (PLQY) of each donor (TTA emitter). The PLQY values were summarized in **Table S2**. The plot indicates parabolic tendency between the luminescence efficiencies versus E_{CT} and that there is an optimal CT energy for efficient luminescence.

To discuss the energetics of the electron transfer in detail, it is necessary to consider the energy offset between the CT state and T_1 rather than the absolute value of CT state energy. To obtain the energy level of T_1 in a situation similar to the real device, i.e. solid state at room temperature, we investigated the phosphorescent spectra from anthracene derivatives under different temperatures. T_1 of the anthracenes was sensitized by triplet sensitizer (PtOEP)[36] because intersystem crossing from S_1 to T_1 rarely occurs in the neat anthracene films. The energy of T_1 is calculated from the peak wavelength of the phosphorescent spectrum. The phosphorescent spectra from the anthracene are shown in **Fig. 3d**. The phosphorescence from the anthracene films appears at about 700 nm (1.76 eV) in 77 K. From the temperature dependence of phosphorescent spectra (**Fig. S12**), T_1 levels at device

operating temperature (300 K) for all three donors (TTA emitters), which are almost the same, approximately 1.65 eV, were obtained by extrapolation to 300 K as shown in **Fig. 3e**.

We then compared the device properties of all the 45 combinations in terms of energy offset. **Fig. 3f** shows the relation between the luminescence efficiency and energy offset ($E_{CT} - E_{T_1}$). The closer $E_{CT} - E_{T_1}$ is to 0, that is, the closer the CT state energy is to the T_1 energy, the higher the luminescence efficiency tends to be. However, the plot is scattered, that is, some combinations of materials have luminescence efficiencies that differ by more than one order of magnitude, despite having similar CT state and T_1 energy differences.

To reveal the reason for the deviation in **Fig. 3d**, we focused on the D/A interaction governed by the structural factor at the interface. the D/A interfacial properties, including the strength of the CT interaction, D/A distance, and molecular orientation, are considered to have a significant effect on electron transfer[15]. These parameters are reflected in the electronic coupling matrix element (H_{DA}) between the electron donor and acceptor. In general, large electronic coupling will facilitate the electron transfer[37]. To evaluate the electronic coupling at the D/A interface, we focused on the absorption of the CT state measured by using the highly sensitive incident photon-to-current conversion efficiency (IPCE). CT absorption intensity is proportional to the square of the electronic coupling matrix element (H_{DA}) at the interface based on the theory of the CT state proposed by Vandewal *et al*[38]. In our system, CT absorption was observed at approximately 2.0–2.4 eV (**Fig. 4a-c**). The intensity of CT absorption was estimated by Gaussian fitting of IPCE spectra[38]. The number

of the order of CT absorption strength is listed on the parabolic plots of luminescence efficiency versus energy offset of 45 devices, as displayed in **Fig. 4d** and **Table S3**. Those with a lower numbers tend to be at the top of the graph for a similar energy gap (e.g. No.1: 1,2-ADN/HF and No.2: PCAN/Cy), and vice versa (e.g. No.32: TPA-An-mPhCz/EH and No.45: 1,2-ADN/TbPh). The results indicate that larger electronic coupling, that is, stronger D/A interaction facilitates electron transfer.

The rate constant of electron transfer (k_{ET}) is commonly discussed by semi-classical Marcus theory[37]. In semi-classical Marcus theory, low-frequency vibrations around molecules are treated classically, while high-frequency internal vibrational modes are treated in a quantum manner as follows.

$$k_{ET} = \frac{2\pi}{\hbar} \frac{{H_{DA}}^2}{\sqrt{4\pi\lambda k_B T}} \sum_{w=0}^{\infty} \frac{e^{-S} S^w}{w!} \exp\left(\frac{-(\Delta G + \lambda + w\hbar\nu)^2}{4\lambda k_B T}\right) \quad (1)$$

k_{ET} is proportional to the square of the electronic coupling matrix element (H_{DA}). Therefore, dividing the EQE_{max} by the CT absorption intensity can be regarded as leveling the electronic coupling between different material combinations and extracting the normalized electron transfer efficiency versus energy offset. In other words, it means to extract the contribution of the energy term of Marcus theory on electron transfer. See supplementary information for detailed discussion.

Dividing the y-axis of **Fig. 4d** by the CT absorption intensity yielded a new plot, **Fig. 4e**, showing a relation of the normalized electron transfer efficiency from the CT state to T_1 on the energy difference of the states. The relation between electron transfer efficiency can be seen to be an

upward convex parabola. When $E_{CT} < E_{T_1}$, that is, the CT state energy is smaller than T_1 of the emitter, the electron transfer efficiency increases as the CT state energy increases. This behavior corresponds to the normal region of the Marcus theory. Activation-less electron transfer occurs when the parabola is close to its maximum, i.e. $E_{CT} \approx E_{T_1}$. In contrast, the efficiency of electron transfer decreases as the CT state energy increases when the CT state energy is larger than T_1 of the emitter. This can be explained by the inverted region of the Marcus theory. The parabolic plot of the electron transfer efficiency in **Fig. 4e** was fitted based on the semi-classical Marcus theory, explaining the experimental results well with a reorganization energy $\lambda = 0.08$. For other parameters and fitting details, see supplementary information. This small reorganization energy of < 0.1 eV means that the electron transfer is facilitated by a minimal energy offset of less than 0.1 eV. Reducing the energy offset for the electron transfer steps in the OLED is critical because the offset is directly added to the extra driving voltage for the emission. The fact that the electron transfer is accelerated by minimal energy offsets is a great advantage for operating the UC-OLED under extremely low driving voltage.

Furthermore, the electron transfer step is involved in the photon upconversion (PUC) which is the process of converting from lower-energy (longer-wavelength) light to higher-energy (shorter-wavelength) light. We reported a novel PUC mechanism using TTA from the electron transfer from CT to T_1 originating from photogenerated free charges[39]. To verify the generality of our result, we also fabricated and analyzed five devices consisting of rubrene and ITIC derivatives. These combinations are reported to be used in PUCs[39]. Rubrene is known as the most widely used yellow

TTA emitter[32]. ITIC derivatives with different substituents have different LUMO levels[40–42] and can therefore vary their CT levels (**Fig. S2**). Since the PUC efficiency is strongly influenced by the charge separation efficiency, we discuss here in terms of the luminescence efficiency using injected charge from the electrode. In these rubrene systems, the luminescence efficiency decreased as the CT energy moved away from the triplet energy of the emitter. The detail of device properties is summarized in the supplementary information. This result further supports our discussion that the electron transfer is facilitated by a smaller energy offset. Reducing energy offset is also important for PUCs to maximize optical energy gain.

Electron transfer from the CT state to T_1 plays an essential role not only in emitting devices such as UC-OLEDs and PUCs, but also in OPVs. Gillett, Nguyen, Beljonne and Friend *et al.* reported that the last challenge in OPVs is to suppress the non-radiative energy loss derived from the electron transfer from the CT state to T_1 of the non-fullerene acceptor[26]. According to their calculations, the suppression of this loss pathway enables the power conversion efficiency (PCE) of more than 20%, typical for inorganic PVs, to be achieved by reducing open-circuit voltage loss. In contrast to our UC-OLED system, the electron transfer from the CT state to T_1 must be suppressed to further improve the PCE of OPV. Based on our analysis, we propose a novel strategy for suppressing non-radiative recombination. Now, if we want to suppress the electron transfer to 1/100, there are two strategies. The first strategy is to raise the level of the T_1 about 0.2 eV above the CT state energy. This corresponds to the normal region in Marcus theory. However, this situation is difficult to realize

in terms of molecular design because T_1 of NFA should be higher than the CT state. This implies that the singlet-triplet energy gap should become almost zero, similar to the behavior observed in the thermally activated delayed fluorescence (TADF) molecules[43]. An alternative solution is to lower the T_1 energy about 0.4 eV below the CT state energy. This is the inverted region in Marcus theory. The reason for the requirement for a larger energy offset in the inverted region than in the normal region is a contribution of molecular vibration with a larger quantum number in semi-classical Marcus theory.

PCAN/PhE is the best D/A combination showing the highest luminescence efficiency due to the optimal E_{CT} and strong D/A interaction for efficient transition from CT state to T_1. To optimize the PCAN/PhE-based device, 2,5,8,11-tetra-*tert*-butylperylene (TbPe), known as a typical blue fluorescent material[44], is doped into the PCAN emission layer. The optimized device structure was depicted in **Fig. 5a**. The undoped PCAN thin layer next to the MoO_3 layer and the acceptor layer inhibits the interfacial quenching of the S_1 exciton on TbPe[23,24,31], and the final emission from TbPe occurs apart from the interface. The *J*-*V* and *L*-*V* curves of the optimized thin layer device were shown in **Fig. 5b**. The voltage that shows 100 cd/m^2, which is equivalent to the luminance of a typical smartphone display, was 1.99 V. The blue emission from the UC-OLED can be observed only by connecting a 1.5 V battery as shown in the inset of **Fig. 5b**. More importantly, the maximum EQE of the optimized device achieved 4.04% with a peak wavelength of 462 nm (**Fig. 5c**). The EQEs of blue OLED devices with turn-on voltages below 2.4 V including not only the UC-OLED

but also the conventional mechanisms[23,31,45,46] are summarized in **Fig. 5d**. To the best of our knowledge, this EQE of 4.04% is the highest value reported to date.

Conclusion

In summary, we have demonstrated the enhancement of electron transfer from the CT state to T_1 by the minimal energy offset through the analysis of the 45 combinations of UC-OLEDs consisting of 3 donors (TTA emitters) and 15 acceptors. This behavior can be explained by the semi-classical Marcus theory with small reorganization energy ($\lambda < 0.1$ eV) by considering the information at the D/A interface, specifically the electronic coupling. Based on our analysis, we have found a novel combination of donor and acceptor. After optimizing the device structure, we have achieved an EQE of more than 4% at a peak wavelength of 462 nm (2.68 eV). This value is the highest EQE among blue OLEDs with turn-on voltages below 2.4 V. Our findings contribute for understanding underlying mechanisms of electron transfer from CT state to T_1, relating not only to improve the efficiency of UC-OLEDs and PUCs but also to suppress the non-radiative recombination in the OPV. We believe that precise control of energetics and structural factors of the D/A interface will drastically enhance the electron transfer processes, leading to the development of efficient organic optoelectronic devices.

Data Availability

The main data supporting the findings of this study are available within the article and its Supplementary Information. Extra data are available from the corresponding authors on request.

Acknowledgements

This research was supported in part by JSPS KAKENHI, Grants-in-Aid for Scientific Research (21H05411, 22K14592), JST PRESTO (JPMJPR2101), JST A-STEP (JPMJTR23R8) and The Morino Foundation for Molecular Science. The authors would like to thank K. Tajima and K. Nakano at RIKEN for their assistance with the photoelectron yield measurements. The authors would like to thank R. Kani for his assistance with phosphorescence measurements. H. I. would like to thank financial support from Fuji Seal Foundation.

Author Contributions

H. I. and S. I. conceived the idea, designed the experiment, and wrote the paper. H. I. fabricated the OLED devices and conducted the OLED characterization. K. F. and K. B. designed and synthesized NDI derivatives. Q. S. synthesized TPA-An-mPhCz. Y. M. and M. T. supervised the research. S.I. directed the project. All the authors reviewed the manuscript.

Competing Interests

The authors declare no competing interest.

References

1. Marcus, R. A., Sutin, N. & Amos, A. *Electron Transfers in Chemistry and Biology*. *Biochimica et Biophysica Acta* **811**, 265-322 (1985).
2. Romero, N. A. & Nicewicz, D. A. Organic Photoredox Catalysis. *Chemical Reviews* **116**, 10075–10166 (2016).
3. Kordt, P. *et al.* Modeling of Organic Light Emitting Diodes: From Molecular to Device Properties. *Advanced Functional Materials* **25**, 1955–1971 (2015).
4. Thompson, B. C. & Fréchet, J. M. J. Polymer-fullerene composite solar cells. *Angewandte Chemie - International Edition* **47**, 58–77 (2008).
5. Moser, C., Keske, J., Warncke, K. *et al*. Nature of biological electron transfer. *Nature* **355**, 796–802 (1992).
6. Douglas R. Green, John C. Reed Mitochondria and Apoptosis. *Science* **281**,1309-1312 (1998).
7. Marcus, R. A. Electron Transfer Reactions in Chemistry: Theory and Experiment (Nobel Lecture). *Angewandte Chemie International Edition* **32**, 1111–1121 (1993).
8. Marcus, R. A. On the theory of chemiluminescent electron-transfer reactions. *J Chem Phys* **43**, 2654–2657 (1965).
9. Marcus, R. A. On the Theory of Electron-Transfer Reactions. VI. Unified Treatment for Homogeneous and Electrode Reactions. *J Chem Phys* **43**, 679–701 (1965).
10. Huang, Y., Hsiang, E. L., Deng, M. Y. & Wu, S. T. Mini-LED, Micro-LED and OLED displays: present status and future perspectives. *Light: Science and Applications* **9**, 105 (2020).
11. Wadsworth, A. *et al.* Critical review of the molecular design progress in non-fullerene electron acceptors towards commercially viable organic solar cells. *Chemical Society Reviews* **48**, 1596–1625 (2019).
12. Lee, J. H. *et al.* Blue organic light-emitting diodes: Current status, challenges, and future outlook. *Journal of Materials Chemistry C* **7**, 5874–5888 (2019).
13. Hoppe, H. & Sariciftci, N. S. Organic solar cells: An overview. *J Mater Res* **19**, 1924–1945 (2004).
14. Vandewal, K. Interfacial Charge Transfer States in Condensed Phase Systems. *Annu Rev Phys Chem* **67**, 113–133 (2016).
15. Zhu, X. Y., Yang, Q. & Muntwiler, M. Charge-transfer excitons at organic semiconductor surfaces and interfaces. *Acc Chem Res* **42**, 1779–1787 (2009).

16. Izawa, S., Nakano, K., Suzuki, K., Hashimoto, K. & Tajima, K. Dominant effects of first monolayer energetics at donor/acceptor interfaces on organic photovoltaics. *Advanced Materials* **27**, 3025–3031 (2015).
17. Sarma, M. & Wong, K. T. Exciplex: An Intermolecular Charge-Transfer Approach for TADF. *ACS Appl Mater Interfaces* **10**, 19279–19304 (2018).
18. Friederich, P. *et al.* Toward Design of Novel Materials for Organic Electronics. *Advanced Materials* **31**, (2019).
19. Janssen, R. A. J. & Nelson, J. Factors limiting device efficiency in organic photovoltaics. *Advanced Materials* **25**, 1847–1858 (2013).
20. Chow, P. C. Y. *et al.* Factors That Prevent Spin-Triplet Recombination in Non-fullerene Organic Photovoltaics. *Journal of Physical Chemistry Letters* **12**, 5045–5051 (2021).
21. Zhou, G. *et al.* Marcus Hole Transfer Governs Charge Generation and Device Operation in Nonfullerene Organic Solar Cells. *ACS Energy Lett* **6**, 2971–2981 (2021).
22. Shuai, Z., Li, W., Ren, J., Jiang, Y. & Geng, H. Applying Marcus theory to describe the carrier transports in organic semiconductors: Limitations and beyond. *Journal of Chemical Physics* **153**, 080902 (2020).
23. Izawa, S. *et al.* Blue organic light-emitting diode with a turn-on voltage of 1.47 V. *Nat Commun* **14**, 5494 (2023).
24. Izawa, S., Morimoto, M., Naka, S. & Hiramoto, M. Efficient Interfacial Upconversion Enabling Bright Emission at an Extremely Low Driving Voltage in Organic Light-Emitting Diodes. *Adv Opt Mater* **10**, (2022).
25. Scholz, S., Kondakov, D., Lüssem, B. & Leo, K. Degradation mechanisms and reactions in organic light-emitting devices. *Chemical Reviews* **115**, 8449–8503 (2015).
26. Gillett, A. J. *et al.* The role of charge recombination to triplet excitons in organic solar cells. *Nature* **597**, 666–671 (2021).
27. Scharber, M. C. *et al.* Design rules for donors in bulk-heterojunction solar cells - Towards 10 % energy-conversion efficiency. *Advanced Materials* **18**, 789–794 (2006).
28. Sasaki, T. *et al.* Unravelling the electron injection/transport mechanism in organic light-emitting diodes. *Nat Commun* **12**, 2706 (2021).
29. Cho, I., Kim, S. H., Kim, J. H., Park, S. & Park, S. Y. Highly efficient and stable deep-blue emitting anthracene-derived molecular glass for versatile types of non-doped OLED applications. *J Mater Chem* **22**, 123–129 (2012).
30. Han, P. *et al.* Aggregation-induced emission luminogen with excellent triplet-triplet upconversion efficiency for highly efficient non-doped blue organic light-emitting diodes. *Mater Horiz* **9**, 376–382 (2022).
31. Lin, B. Y. *et al.* Exciplex-Sensitized Triplet-Triplet Annihilation in Heterojunction Organic Thin-Film. *ACS Appl Mater Interfaces* **9**, 10963–10970 (2017).

32. Zhou, J., Liu, Q., Feng, W., Sun, Y. & Li, F. Upconversion luminescent materials: Advances and applications. *Chemical Reviews* **115**, 395–465 (2015).
33. Yanai, N. & Kimizuka, N. New Triplet Sensitization Routes for Photon Upconversion: Thermally Activated Delayed Fluorescence Molecules, Inorganic Nanocrystals, and Singlet-to-Triplet Absorption. *Acc Chem Res* **50**, 2487–2495 (2017).
34. Zhang, G. *et al.* Nonfullerene Acceptor Molecules for Bulk Heterojunction Organic Solar Cells. *Chemical Reviews* **118**, 3447–3507 (2018).
35. Monguzzi, A., Mézyk, J., Scotognella, F., Tubino, R. & Meinardi, F. Upconversion-induced fluorescence in multicomponent systems: Steady-state excitation power threshold. *Phys Rev B Condens Matter Mater Phys* **78**, 195112 (2008).
36. Shukla, A. *et al.* Controlling triplet–triplet upconversion and singlet-triplet annihilation in organic light-emitting diodes for injection lasing. *Commun Mater* **3**, 27 (2022).
37. Jortner, J. Temperature dependent activation energy for electron transfer between biological molecules. *J Chem Phys* **64**, 4860–4867 (1976).
38. Vandewal, K., Tvingstedt, K., Gadisa, A., Inganäs, O. & Manca, J. V. Relating the open-circuit voltage to interface molecular properties of donor:acceptor bulk heterojunction solar cells. *Phys Rev B Condens Matter Mater Phys* **81**, 125204 (2010).
39. Izawa, S. & Hiramoto, M. Efficient solid-state photon upconversion enabled by triplet formation at an organic semiconductor interface. *Nat Photonics* **15**, 895–900 (2021).
40. Li, S. *et al.* Energy-Level Modulation of Small-Molecule Electron Acceptors to Achieve over 12% Efficiency in Polymer Solar Cells. *Advanced Materials* **28**, 9423–9429 (2016).
41. Laventure, A. & Welch, G. C. A tetrachlorinated molecular non-fullerene acceptor for high performance near-IR absorbing organic solar cells. *J Mater Chem C Mater* **6**, 9060–9064 (2018).
42. Zhao, W. *et al.* Molecular Optimization Enables over 13% Efficiency in Organic Solar Cells. *J Am Chem Soc* **139**, 7148–7151 (2017).
43. Uoyama, H., Goushi, K., Shizu, K. *et al*. Highly efficient organic light-emitting diodes from delayed fluorescence. *Nature* **492**, 234–238 (2012)
44. Kim, S.-K. *et al.* New Blue and Bluish Green Electroluminescent Properties of Fully Substituted Ethylene Moieties. *Molecular Crystals and Liquid Crystals* **462**, 209–216 (2006).
45. Satoh, C. *et al.* Bandgap Engineering for Ultralow-Voltage Operation of Organic Light-Emitting Diodes. *Adv Opt Mater* **11**, 2300683. (2023)
46. Kakumachi, S., Ba Nguyen, T., Nakanotani, H. & Adachi, C. Abrupt exciton quenching in blue fluorescent organic light-emitting diodes around turn-on voltage region. *Chemical Engineering Journal* **471**, 144516 (2023).

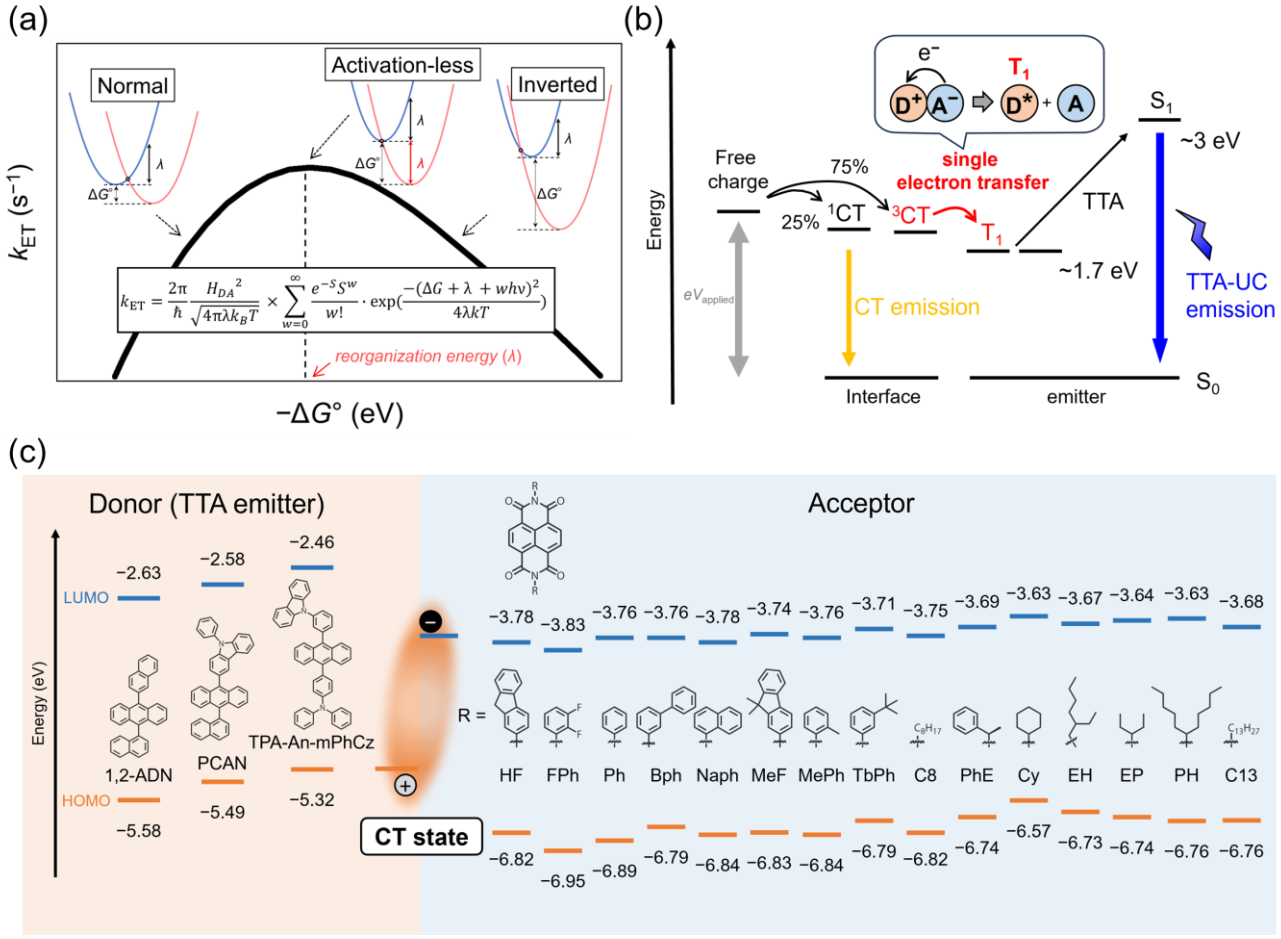

Fig. 1 a) Conceptual illustration and the equation of semi-classical Marcus theory. The blue line and red line describe Gibbs energy surface of the reactant and product, respectively. b) Schematic of the mechanism of blue UC-OLEDs. c) Chemical structures and energy levels of the materials used in this study and conceptual image of CT formation. HOMO of donors (TTA emitters) and LUMO of acceptors were measured by cyclic voltammetry (CV), while LUMO of donors and HOMO of acceptors were calculated from their optical band gap and CV results.

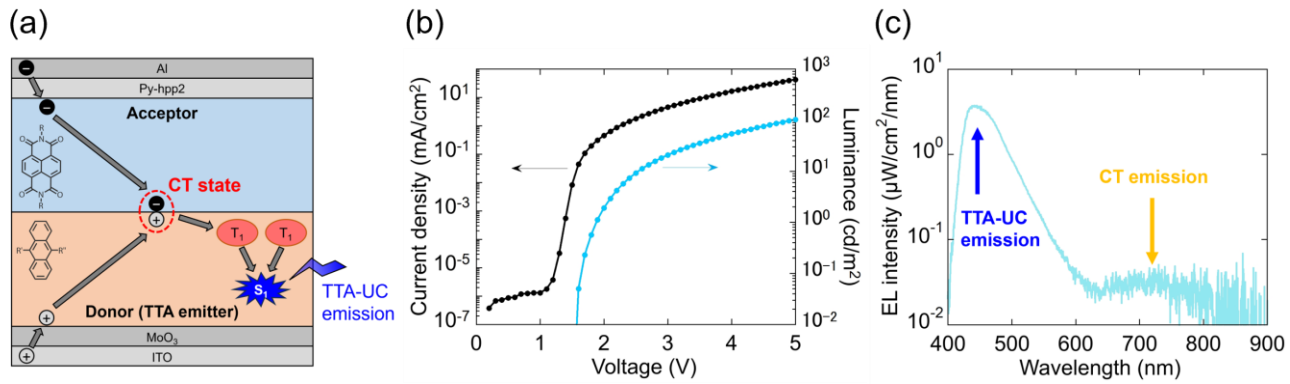

Fig. 2 a) Device structure and schematic of UC-OLEDs. b) *J*-*V* and *L*-*V* curves of PCAN/PhE-based device. c) EL spectrum of the PCAN/NDI-PhE-based device under a constant current flow (100 mA/cm^2).

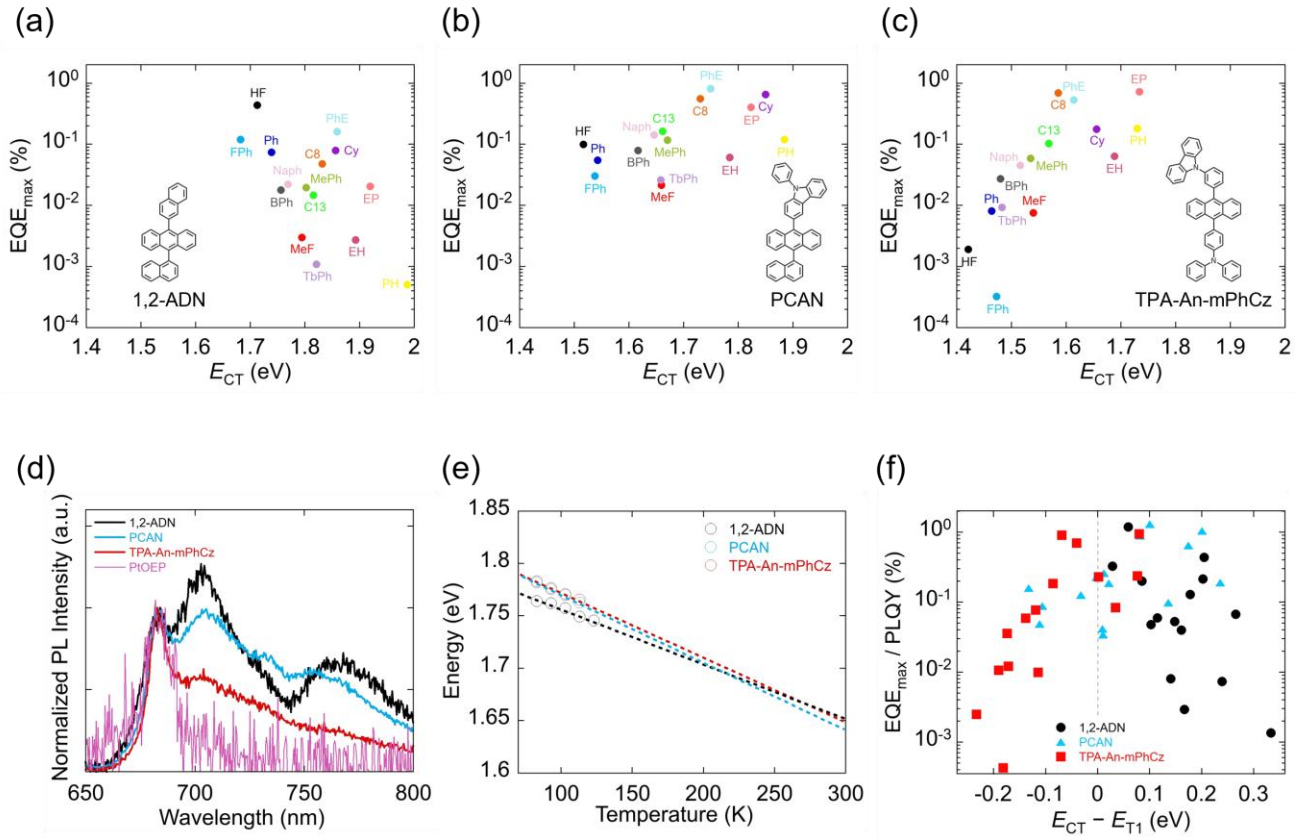

Fig. 3 a, b, c) Correlation between the energy of the CT states and their maximum EQE of the (a) 1,2-ADN/acceptor-based, (b) PCAN/acceptor-based and (c) TPA-An-mPhCz/acceptor-based devices. d) Phosphorescent spectra of PtOEP doped 1,2-ADN (black), PCAN (sky blue), TPA-An-mPhCz (red), and PtOEP neat film with excitation wave length of 550 nm at 77 K. e) Temperature dependent energies of phosphoresce of PtOEP doped 1,2-ADN (black), PCAN (sky blue), TPA-An-mPhCz (red), and PtOEP neat film with excitation wave length of 550 nm. The broken lines describe extrapolation lines of each donor (TTA emitter). f) Correlation between the $E_{\mathrm{CT}} - E_{\mathrm{T_1}}$ and the maximum EQE divided by PLQY of each donor (TTA emitter)

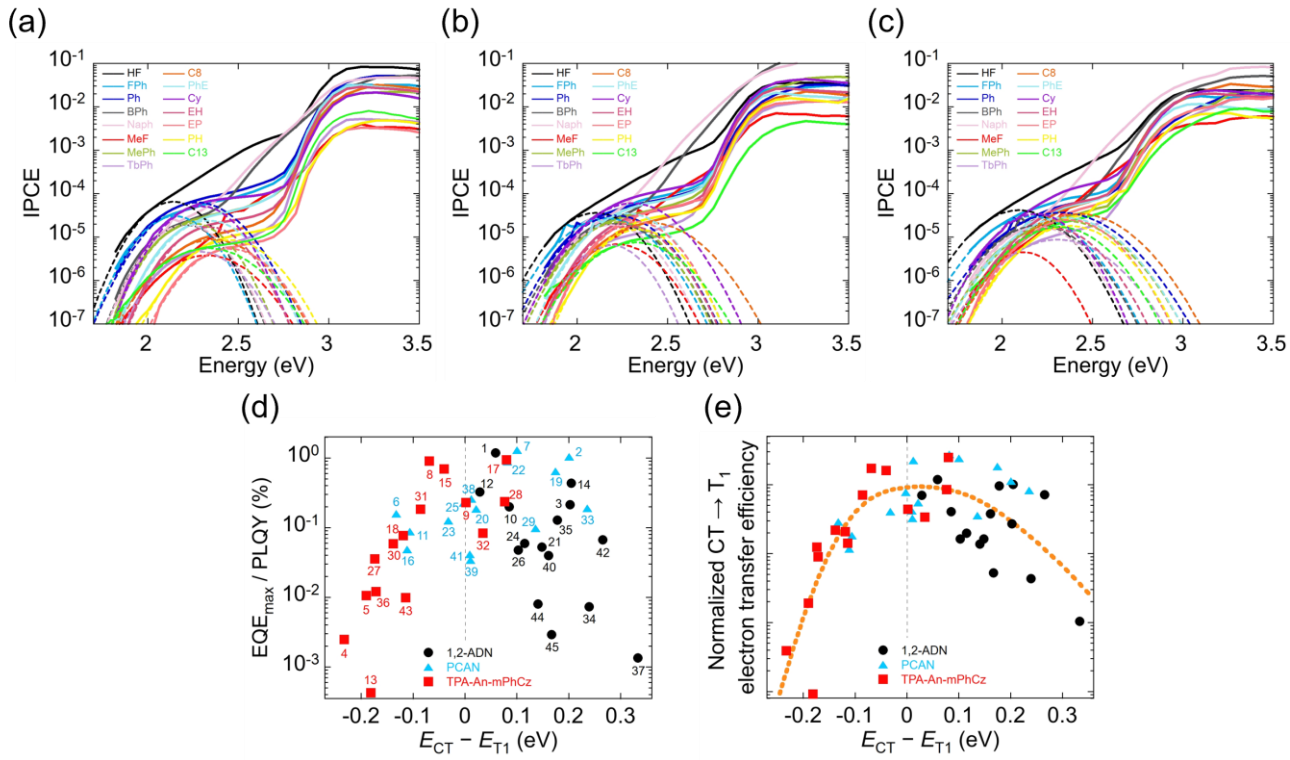

Fig. 4. a, b, c) IPCE spectra of their fitting curves of the (a) 1,2-ADN/acceptor, (b) PCAN/acceptor and (c) TPA-An-mPhCz/acceptor devices. d) Correlation between the $E_{CT} - E_{T_1}$ and the maximum EQE divided by PLQY of each donor (TTA emitter). The numbers in the graph show the order of CT absorption strength. e) Correlation between the $E_{CT} - E_{T_1}$ and the normalized electron transfer efficiency from CT state to T_1 and fitted curve using semi-classical Marcus theory with reorganization energy λ = 0.08. See main text and supplementary information for further information.

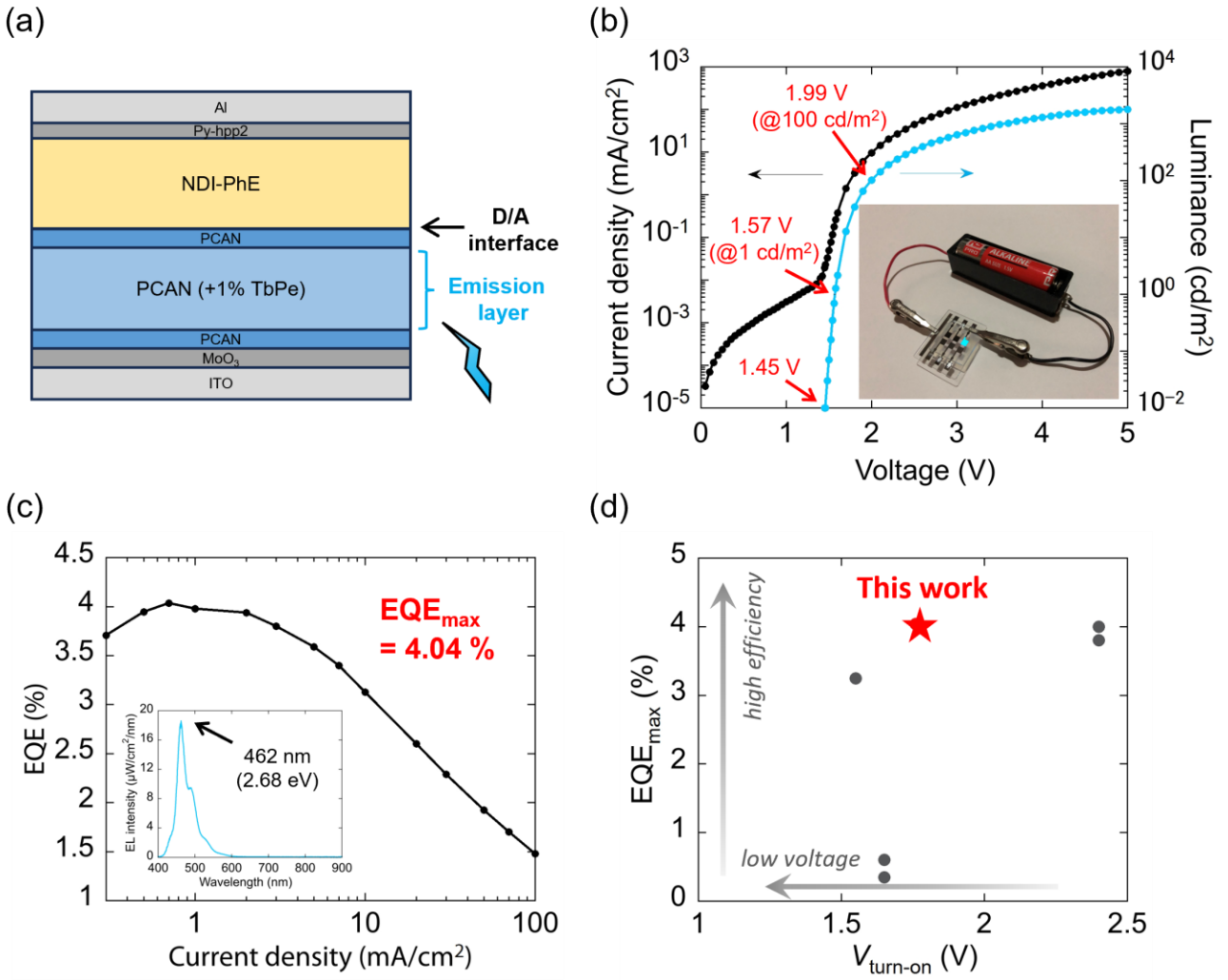

Fig. 5 a) Optimized device structure using TbPe as fluorescent dopant. b) *J-V* and *L-V* curves of the optimized thin layer PCAN/PhE-based device. Inset: photograph of the device operated by only a 1.5 V battery. c) EQE of the optimized PCAN/PhE-based device. Inset: EL emission spectrum of the optimized device under a constant current flow (100 mA/cm^2). d) Maximum EQE versus turn-on voltage of reported blue (peak wavelength λ, 430 < λ < 470 nm) OLED with turn-on voltage below 2.4 V reported to date.